



**Comparative life cycle assessment of corn stover conversion  
by decentralized biomass pyrolysis-electrocatalytic  
hydrogenation versus ethanol fermentation**

Journal:	<i>Sustainable Energy &amp; Fuels</i>
Manuscript ID	SE-ART-01-2022-000055.R2
Article Type:	Paper
Date Submitted by the Author:	05-Dec-2022
Complete List of Authors:	Das, Sabyasachi; Michigan State University Anderson, James; Ford Motor Company, Research & Advanced Engineering De Kleine, Robert; Ford Motor Company, Advanced Engineering 2101 Village Road Wallington, Timothy; Ford Motor Company, Research & Advanced Engineering Jackson, James; Michigan State University, Chemistry Saffron, Christopher; Michigan State University, Biosystems and Agricultural Engineering, Chemical Engineering and Material Science

# Comparative life cycle assessment of corn stover conversion by decentralized biomass pyrolysis-electrocatalytic hydrogenation versus ethanol fermentation

Sabyasachi Das<sup>a</sup>, James E. Anderson<sup>b</sup>, Robert De Kleine<sup>b</sup>, Timothy J. Wallington<sup>b</sup>, James E. Jackson<sup>c</sup>, Christopher M. Saffron<sup>a,d\*</sup>

<sup>a</sup>*Department of Chemical Engineering and Materials Science, Michigan State University, East Lansing, Michigan 48824, USA*

<sup>b</sup>*Research and Advanced Engineering, Ford Motor Company, Dearborn, MI 48121, USA*

<sup>c</sup>*Department of Chemistry, Michigan State University, East Lansing, MI 48824, USA*

<sup>d</sup>*Department of Biosystems and Agricultural Engineering, Michigan State University, East Lansing, MI 48824, USA*

## Abstract:

Quantification of environmental impacts through life cycle assessment is essential when evaluating bioenergy systems as potential replacements for fossil-based energy systems. Bioenergy systems employing localized fast pyrolysis combined with electrocatalytic hydrogenation followed by centralized hydroprocessing (Py-ECH) can have higher carbon and energy efficiencies than traditional cellulosic biorefineries. A cradle-to-grave life cycle assessment was performed to compare the performance of Py-ECH versus cellulosic fermentation in three environmental impact categories: climate change, water scarcity, and eutrophication. Liquid hydrocarbon production using Py-ECH was found to have much lower eutrophication potential and water scarcity footprint than cellulosic ethanol production. Greater amounts of renewable electricity led to lower greenhouse gas emissions for the Py-ECH processing. When the renewable fraction of grid electricity is higher than 87%, liquid hydrocarbon production using Py-ECH has lower greenhouse gas emissions than cellulosic ethanol production. A sensitivity analysis illustrates the major role of annual soil carbon sequestration in determining system-wide net greenhouse gas emissions.

## 1. Introduction

Production and combustion of fossil fuels, such as liquid fuels derived from crude oil, are significant contributors to air and water pollution and contribute to global warming. Such fuels are non-renewable as the rate of replenishment is much slower than the rate of depletion. There is a need to look for alternative energy production systems that are renewable and less polluting. The

U.S. Energy Independence and Security Act (EISA),<sup>1</sup> passed in 2007, aims to increase the production of cleaner renewable fuels, as part of the overall mission of improving energy security. The EISA promotes the production of biofuels as a cleaner and renewable alternative to fossil fuels by requiring the use of at least 21 billion gallons of advanced biofuels (with 16 billion gallons of cellulosic biofuels) by the year 2022. In accordance with EISA, these advanced biofuels must provide at least a 50% reduction in greenhouse gas emissions compared to the baseline established in 2005.

Fermentation of lignocellulose-derived sugars into ethanol is the most studied advanced biofuel system.<sup>2-5</sup> The process has been commercially implemented in different countries around the world.<sup>6, 7</sup> One such example is the recently inaugurated Clariant plant in Romania that is set to produce 50,000 tons of bioethanol from wheat straw annually.<sup>8</sup> However, traditional cellulosic ethanol systems are inherently carbon and energy inefficient as one-third of the biomass carbon is lost as carbon dioxide and the process typically does not convert the lignin (accounting for 40% of biomass energy)<sup>9</sup> into liquid fuel. These inefficiencies are significant opportunities for improved biofuel yield.<sup>10</sup> Furthermore, significant challenges remain that hinder the widespread commercialization of the technology.<sup>6, 7</sup> While biomass is a considerable energy resource in the U.S., the future demand for biobased energy will be greater<sup>10</sup> and will require optimal use of renewable resources. This was the motivation for our previous work in which we discussed the concept of a bioenergy system with decentralized pyrolysis and electrocatalytic hydrogenation and centralized hydroprocessing (Py-ECH) and established its advantages in carbon and energy efficiency when compared to traditional cellulosic fermentation to ethanol.<sup>11</sup> Research and development has been conducted to support the commercialization of biomass fast pyrolysis to produce bio-oil.<sup>12</sup> The Py-ECH system combines localized fast pyrolysis and subsequent electrocatalytic hydrogenation (ECH)<sup>13-21</sup> with centralized petroleum refinery-style hydroprocessing to produce “drop-in” liquid hydrocarbon fuels. While fast pyrolysis deconstructs the biomass to liquid bio-oil, solid biochar, and non-condensable gases, ECH employs mild conditions to hydrogenate and upgrade the energy content of the bio-oil so that it is stable for storage and transport to a central refinery. At the refinery, the stable bio-oil is subjected to high temperatures and pressures in the presence of hydrogen gas to produce liquid gasoline and/or diesel-range hydrocarbons.<sup>22</sup> In the Py-ECH system, this hydrogen gas is generated from electrolysis at the refinery. Corn stover was selected as the feedstock for the analysis, allowing

comparison with the cellulosic ethanol (CE) process as documented by Humbird et al. in a National Renewable Energy Laboratory (NREL) study.<sup>2</sup> Technoeconomic analysis showed a minimum fuel selling price (MFSP) of \$3.62/gge<sup>23</sup> (in 2018\$, for a fixed internal rate of return of 10%) for Py-ECH compared to \$3.70/gge for CE.<sup>2</sup> However, with improvements in technology, the MFSP for the Py-ECH system could drop to approximately \$3/gge.<sup>23</sup>

Though many life cycle assessments (LCAs) have already been conducted for CE using different biomass feedstocks,<sup>24-31</sup> this exercise was repeated here while maintaining consistent assumptions for the two systems under consideration. Our primary goal is to compare the two technologies under study, namely, Py-ECH and CE, by conducting a full cradle-to-grave analysis, including corn cultivation through end-use fuel combustion in vehicles. Previous LCA studies have demonstrated the environmental advantages of CE systems over fossil fuel systems. Greenhouse gas emissions for CE are 14-16% of the emissions attributed to gasoline from crude oil.<sup>32</sup> Life cycle analyses have also previously been performed for biomass pyrolysis (followed by upgrading using hydrogen gas from different sources) and compared to fossil fuel systems.<sup>33, 34</sup> Similarly, a recent life cycle analysis on a depot-based bioenergy system has shown a pathway to carbon negative cellulosic biofuels.<sup>35</sup> The Py-ECH system, however, integrates decentralized biomass pyrolysis and electrocatalytic hydrogenation with centralized hydroprocessing and refining. Building upon our previous assessments of energy and carbon yield<sup>11</sup> and economics,<sup>23</sup> we present here the LCA environmental impacts of corn stover conversion to hydrocarbon fuels using Py-ECH compared to cellulosic fermentation to ethanol. For consistency with our economic study<sup>23</sup> we consider a decentralized system with densification of biomass to bio-oil and stabilization via ECH at localized (near the biomass) depots. The bio-oil is sufficiently stable to be transported over long distances to a petroleum-style “central” refinery for final upgrading via hydroprocessing.

## 2. Methodology

A comparative “cradle-to-grave” life cycle assessment (LCA) was conducted for the Py-ECH and the CE processes for three environmental impact categories: climate change, water scarcity, and eutrophication. Additionally, the energy return on investment for the two systems was determined to compare their fossil energy footprint. The life cycle inventory was built using data from our previous work<sup>11</sup>, Argonne National Laboratory’s (ANL) GREET<sup>36</sup> and CCLUB<sup>37</sup> models, and a NREL report on cellulosic ethanol.<sup>2</sup>

## 2.1. Functional Unit

Since the primary function of the two bioenergy systems is to produce liquid fuel, the functional unit chosen for the study was 1 MJ of liquid fuel energy to be consumed by an on-road vehicle.

## 2.2. Life Cycle Impact Categories

### *Climate Change/Greenhouse Gas Emissions*

Climate change resulting from anthropogenic emissions primarily of carbon dioxide, but also of methane, nitrous oxide, and halocarbons, is a pressing global sustainability issue. Greenhouse gas (GHG) emissions were determined by calculating the total direct and indirect emissions of carbon dioxide, methane, and nitrous oxide, resulting from all component processes in the scope of study. GHGs were evaluated in units of g CO<sub>2</sub>e/MJ of liquid fuel energy. The emission factors of methane and nitrous oxide were chosen to be 25 and 298 respectively, in accordance with the 100-year time horizon global warming potentials, used in most national and international climate agreements to convert emissions of methane and nitrous oxide into CO<sub>2</sub> equivalents.<sup>38</sup>

### *Water Scarcity*

Bioenergy systems are inherently water intensive and therefore, water consumption is an important parameter. Bayart et al. define freshwater depletion as the “net reduction in the amount/availability of freshwater in a watershed or/and fossil groundwater stock. Depletion occurs when freshwater consumptive use exceeds the renewability rate of the resource over a significant time period.”<sup>39</sup> Boulay et al. developed characterization factors for water use in LCA based on the amount of water remaining in a given watershed per unit area relative to the global average after all human and ecosystem demands have been met.<sup>40</sup> These characterization factors are known as “AWARE” (available water remaining) factors. The Water Scarcity Footprint (WSF) is calculated by multiplying water inventory data with AWARE factors to quantify the potential for depriving another user of water, which is proportional to the water use and inversely proportional to the water availability. The characterization factors range from 0.1 to 100, with 1 for the world average, 0.1 for areas where 10 times more water is available, and 100 for areas with the greatest water scarcity. The average AWARE characterization factors in the United States for agricultural use and non-agricultural use are 36.5 and 9.5, respectively.<sup>41</sup> In the present analysis we used the average

AWARE characterization factors ( $CF_{AWARE}$ ) for the major corn producing states in the Midwest (Minnesota, Wisconsin, North Dakota, South Dakota, Nebraska, and Iowa). These states were chosen for geographical consistency with the Midwest Reliability Organization-West (MROW) e-GRID subregion electrical grid. The average AWARE factors for these states for agricultural and non-agricultural use are 10.2 and 9.6 respectively. Equations 1-3 are used in evaluating the Water Scarcity Footprint (WSF):

$$WSF = w_i \cdot CF_{AWARE} \quad \text{Eq. 1}$$

$$CF_{AWARE} = \frac{1/AMD_i}{1/AMD_{world\ avg}} = \frac{AMD_{world\ avg}}{AMD_i} \quad \text{Eq. 2}$$

$$AMD_i = \frac{(Availability - HWC - EWR)}{Area} \quad \text{Eq. 3}$$

where AMD is availability minus demand ( $m^3$ ), HWC is the human water consumption ( $m^3$ ), EWR is the environmental water requirement ( $m^3$ ), and  $w_i$  is the total inventory of substance  $i$  ( $m^3$ ).

### *Eutrophication*

Biomass production, which is an integral part of all bioenergy systems, depends on the use of fertilizers containing nitrogen, phosphorous, and potassium. These fertilizers are a major source for eutrophication in aquatic systems, which is defined as excess nutrient availability leading to exponential algal and cyanobacteria growth that harms marine systems.<sup>42</sup> The eutrophication potentials for the two systems were estimated using the TRACI Model<sup>43</sup> for 100 year timespans, again in accordance with international climate agreements such as the Paris Agreement and Kyoto Protocol. The TRACI characterization factor for estimating Eutrophication Potential is a combination of a nutrient potency factor and a transport factor.<sup>44</sup> While the potency factor is a measure of the effect of a particular nutrient, the transport factor accounts for the release of emissions into different media (e.g., air, water), ultimately reaching aquatic systems. Equation 4 is used to evaluate the Eutrophication Potential (EUP):

$$EUP_i = \Sigma (e_i \cdot CF_{i,j}) \quad \text{Eq. 4}$$

where  $CF_{i,j}$  is the TRACI characterization factor for substance  $i$  in medium  $j$  (e.g., air and water), and  $e_i$  is the inventory data of substance  $i$  (kg).

### 2.3. System Definition

The results of a life-cycle analysis can vary greatly depending on the establishment of system boundaries. The Py-ECH and CE system boundaries were defined by the cultivation of the corn plant (for generation of stover) in the beginning and by the combustion of the produced hydrocarbon fuel at the end as shown in Figures 1 (a) and (b). The major system components include the feedstock supply, processing at refineries or depots, transport, and fuel combustion. A more detailed Py-ECH system flow diagram is presented in the Supplementary Information of our previous article.<sup>11</sup> For the CE system, similar detailed flow diagrams may be found in the Humbird et al. report.<sup>2</sup>

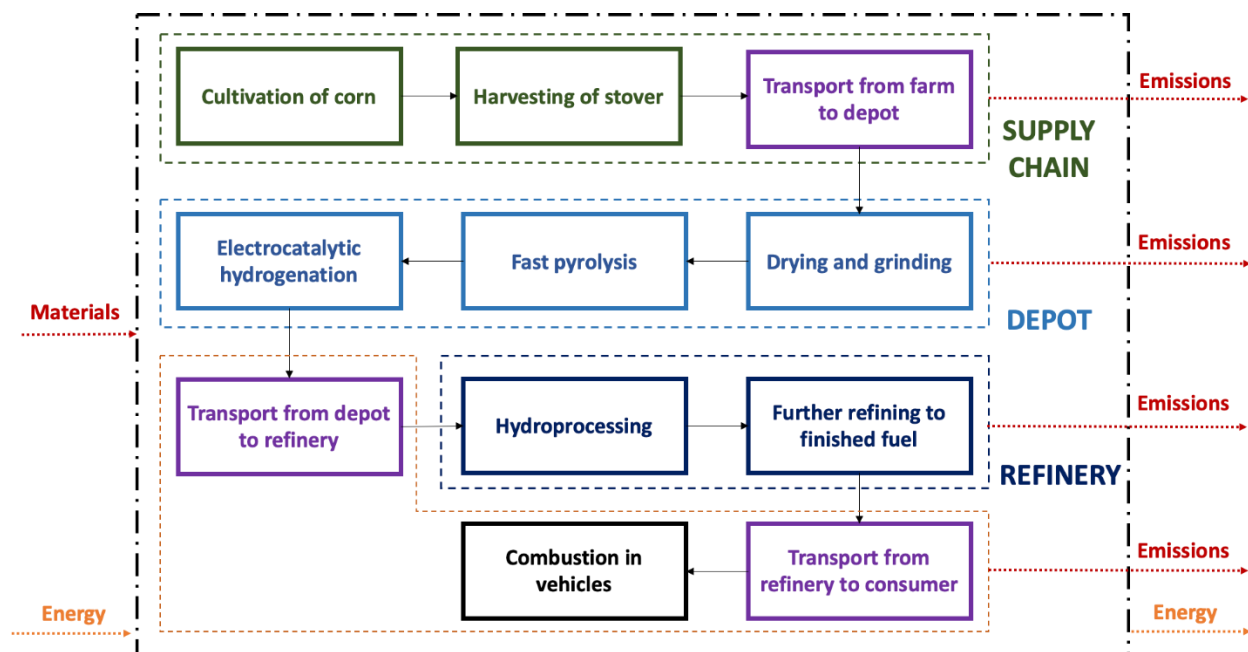


Figure 1 (a): System boundaries for the Py-ECH bioenergy system

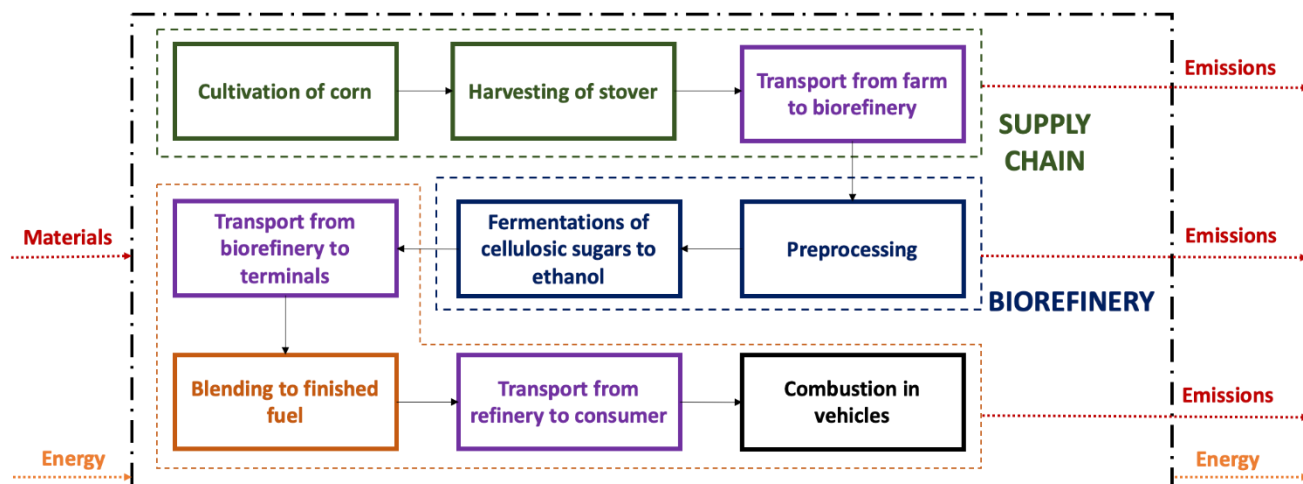


Figure 1 (b): System boundaries for the CE bioenergy system

## 2.4. Time Horizon

A time horizon of 20 years was selected for the LCA to accommodate the transient response of the soil organic matter deposition. Soil organic matter is a measure of soil carbon sequestration, which can serve to off-set greenhouse gas emissions, and may significantly affect the results. Twenty years is sufficient time to account for microbial decomposition and respiration in the soil. Also, a 20-year time horizon aligns with equipment service lifetimes, as employed in technoeconomic analyses.

## 3. Life Cycle Inventory (LCI)

The process flow data for the Py-ECH system were adopted from our previous work, which includes the water, energy, and material consumption data for each unit process as reported in the Supplementary Information of that work.<sup>11</sup> For the CE system, all data were extracted from Humbird et al.<sup>2</sup> Other key LCI data were taken from GREET and CCLUB models. To qualify the collected inventory, data quality indicators (DQI) were assigned using the modified Weidema method.<sup>45</sup> Originally Weidema et al. suggested five parameters to evaluate data quality: reliability, completeness, temporal correlation, geographical correlation, and technological correlation. Toffel et al. replaced the completeness parameter with 'representativeness' and the temporal correlation parameter with 'data age'. They also split the reliability parameter into the acquisition method and independence of data supplier parameters to better characterize the data reliability.<sup>46</sup> This modified Weidema method has been applied in the current study. Table S1 summarizes these parameters



and describes the meaning of the scores assigned to the data on a scale of 1 to 5.<sup>47</sup> All life cycle data used in this study are listed, with their data quality indicators, in Table S2. Key data and assumptions are discussed below for the two bioenergy systems for each of four major areas: feedstock supply, processing, transport, and combustion.

### 3.1. Feedstock Supply

#### *Corn Cultivation*

Data pertaining to the cultivation of corn were obtained from GREET.<sup>36, 37</sup> We assumed that corn is cultivated in a continuous corn cropping system with no tillage. The corn cropland was assumed to be previously used for crops or pasture. It was assumed that 60 wt.% of the generated corn stover was removed from the fields<sup>48</sup> GREET provides two options for stover removal, 60% and 30% by weight. The 60 wt.% stover removal option was selected for high stover yield recognizing that retaining a minimum of 30% corn stover on the field decreases wind erosion (by 70% compared to bare soil).<sup>49</sup> GREET was used for fertilizer data, including emissions from production and soil application. The soil carbon sequestration rate was assumed to be 0.174 Mg C/ha/yr for 60% stover removal (derived from 0.273 Mg C/ha/yr for 30% stover removal in the CCLUB model, 0 Mg C/ha/yr for 100% stover removal,<sup>50</sup> and assuming a linear dependence on stover removal). Carbon sequestration rate is the net accumulation of soil carbon over the selected time horizon, and it accounts for the translocation of photosynthetic carbon, the carbon in root exudates, the carbon deposited in soil organic matter pools, and the carbon liberated as carbon dioxide due to soil respiration and microbial decomposition. Alvarez<sup>51</sup> showed that the rate of soil carbon sequestration is a function of soil texture, rainfall, tillage, stover removal, soil depth measured, crop rotation system, and geographical location. Sequestration rates reported for no-till corn cultivation vary from 0.1 Mg C/ha/yr to about 5 Mg C/ha/yr, depending on these factors.<sup>50, 52-58</sup> Given this wide range, a sensitivity analysis was performed to determine the effect of carbon sequestration rate on GHG emissions.

Figure 2 shows the carbon flow for the CE and Py-ECH systems, assuming 60% stover removal. The carbon flows for both systems are identical, starting with photosynthetic carbon, and only differ in the fate of the processed corn stover. As reported previously,<sup>11</sup> the Py-ECH system directs 2.4 times more biomass carbon to fuel products than the CE system and produces a significant amount of biochar. In the cellulosic ethanol process, less than a third of the corn stover carbon

ends up in the ethanol product, with the remainder lost as CO<sub>2</sub> during fermentation and lignin combustion.

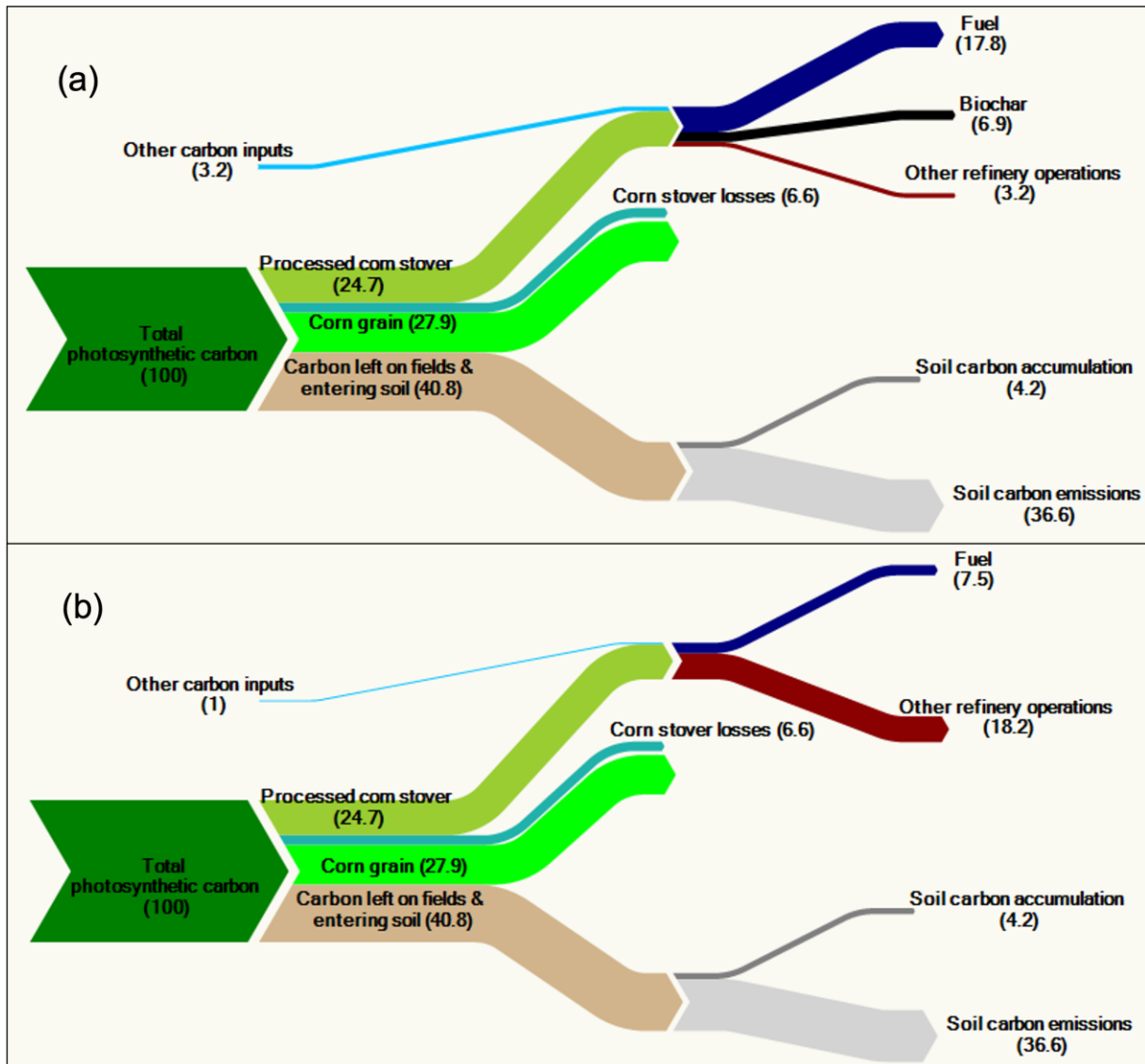


Figure 2: Carbon flow of the (a) Py-ECH and (b) CE systems. All values are percentages of total photosynthetic carbon.

Parameters for amount of water required for cultivation was taken from GREET. Water can be separated into three categories: blue (surface water and ground water), green (water associated with precipitation) and grey (water required to incorporate pollutants being discharged into freshwater bodies).<sup>59</sup> For crop cultivation, GREET only includes blue water consumption, where

consumption is defined as the amount of freshwater used by the process for anthropogenic purposes and not returned due to evapotranspiration or reduced quality.<sup>60</sup> Green water consumption in cultivation may be neglected because it does not affect blue water use,<sup>61-64</sup> assuming that green water consumption does not change due to crop cultivation.<sup>62, 64</sup> Grey water was not considered because its environmental consequences overlap with eutrophication, which is already included in the present study. Atmospheric eutrophication emissions of nitrogen oxides (NO<sub>x</sub>, contributing to eutrophication potential) in the cultivation stage due to fertilizer application and production were extracted from GREET. Ammonia emissions due to volatilization of a fraction of the applied fertilizers were estimated from IPCC data.<sup>65, 66</sup> All three fertilizer nutrients (N, P, K) were considered. Emissions due to N and P fertilizer runoff to water resources were obtained from a comprehensive report published by NREL in 2005,<sup>66</sup> which investigated the environmental impacts of fertilizer usage for corn, soybean, and stover. Nitrogen runoff to surface water was included, but runoff reaching groundwater was assumed negligible due to geographic assumptions. The value for N surface runoff (as nitrates) was fixed at 24% of total fertilizer N added, as assumed in GREET.<sup>66</sup> Phosphorus is assumed to contribute to surface water pollution via runoff. There are negligible quantities of P in the atmosphere<sup>67</sup> and groundwater pollution is assumed negligible due to strong sorption of P to soil minerals. The P runoff (as phosphates) to surface water was assumed to be 7% of the total phosphorus added as fertilizer, based on reported values varying from 1% to 14%.<sup>66</sup> Potassium has minimal contribution to water eutrophication.

### *Collection of Stover*

The three basic operations associated with stover harvesting are windrowing, baling, and collection.<sup>68</sup> A stalk chopper/windrower is used to avoid collecting foreign material with the stover feedstock, baling facilitates collection and transportation, thereby reducing transportation costs.<sup>69, 70</sup> Harvesting equipment (tractors, balers, combines, swathers, sprayers, tillers etc.)<sup>71</sup> consume 3.58 gallons of diesel fuel per acre for full harvest of stover, excluding grain. The emissions associated with diesel combustion were taken from GREET. Stover storage, transportation, and farm handling losses are 8.4%, 2%, and 2% of dry stover, respectively.<sup>36</sup> Emissions from decomposition of lost biomass are dependent<sup>72</sup> on temperature and moisture content<sup>72</sup> and were estimated to be between 2.3 and 8.4 g CO<sub>2</sub> e/MJ of fuel produced for the cellulosic ethanol processes.<sup>73</sup> Based on the ratio of carbon present in the feedstock biomass (on a produced fuel energy basis) an average of 5.35 g

CO<sub>2</sub> e/MJ was computed for the CE system, while a value of 2.3 g CO<sub>2</sub> e/MJ fuel produced was calculated for Py-ECH. These emissions are equal for both processes on a per kg feedstock basis.

### 3.2. Processing

LCI data for electricity and carbon sequestration were obtained from our Py-ECH system model that is based on mass and energy balances.<sup>11</sup> Similarly, data for the CE system were obtained from the Humbird et al. report on cellulosic sugar fermentation to ethanol.<sup>2</sup> For both models, the emissions from electricity generation were estimated using the MROW electrical grid data, which includes the states of Minnesota, Iowa, West Wisconsin, North Dakota, South Dakota, and Nebraska. To estimate the carbon credit from biochar application (for the Py-ECH system only), the biochar was assumed to be 82.5% carbon, based on literature values in the range of 65-100 wt.%.<sup>74, 75</sup> Biochar application has additional soil benefits including decreased fertilizer requirement, reduced NO<sub>x</sub> emissions, and decreased leaching of soil nutrients<sup>76, 77</sup> that leads to decreased emissions. However, these benefits are difficult to estimate and were not considered in this analysis.

Supplemental process heat is required at the central refinery in the Py-ECH system. This heat was assumed to be provided from natural gas with a net heating value of 52.2 MJ/kg. Carbon dioxide emissions from natural gas combustion at the Py-ECH refinery were computed stoichiometrically and associated NO<sub>x</sub> emissions were estimated from GREET. No external heat and power are required by the CE system as it burns the biomass lignin and the wastewater treatment sludge to provide heat and electricity for all plant utilities. Excess electricity is produced and assumed to be sold to the grid, resulting in associated credits for the CE system. The Py-ECH depots are self-sufficient in heat and power requirements owing to combustion of the non-condensable gases (NCG) generated during pyrolysis. NO<sub>x</sub> emissions from burning lignin and sludge for CE, and CNG for Py-ECH, were assumed to be 0.31 kg/MWhr of fuel net heating value.<sup>2</sup>

Regarding water consumption in the CE system, most of the water is recycled by treating wastewater, though well water is consumed to make up for the cooling tower evaporative losses (about 1.2 million cubic meters per year).<sup>2</sup> The Py-ECH system utilizes water predominantly in the ECH and electrolysis units, with a combined total of about 0.2 million cubic meters per year.<sup>11</sup> While most emissions from the processing stages of CE and the Py-ECH are atmospheric in nature,

there is one liquid waste stream (the treated 50% brine solution from the wastewater treatment plant) in the CE system.<sup>2</sup> However, with recent advances in membrane-based and thermal-based technologies for brine treatment, the concept of zero-liquid-discharge systems is fast emerging.<sup>78</sup> Therefore, no liquid discharge stream was assumed in the present analysis. Consequently, no grey water consumption or water eutrophication was considered for the processing stage of either system.

### 3.3. Transport

To model the transportation of corn stover, trailer trucks (53 ft long, 8.5 ft wide, 13.5 ft high) were assumed.<sup>68, 79</sup> The 80,000-lb vehicle weight limit for roadways in Iowa served as a constraint. Assuming the average dry weight of a 3 ft x 5 ft x 8 ft bale to be 950 lbs, the average wet weight for a similarly sized bale with 20% moisture is approximately 1,200 lb.<sup>79</sup> If the weight of the trailer is assumed to be 30,000 lbs, then a maximum of 50,000 lb (48 bales) can be transported per trip. Volume constraints would allow up to 63 bales per trip, hence weight limitation is the limiting constraint. The average corn stover collection radius from the fields to the biorefinery in the CE system is assumed to be 50 miles (80 km) for the assumed biorefinery size.<sup>48</sup> For the Py-ECH system, the modeled distance between the corn fields and upgrading depots is 7 miles (11.5 km) based on an optimization for the lowest cost of finished fuel.<sup>80</sup> This is consistent with literature predictions of distances between 9 and 55 km for optimal transport distance.<sup>81</sup> Similarly, the mean distance from depots to the central refinery was determined as approximately 51 km, by minimizing the final fuel price. The mean distance for transporting the finished fuels from the refinery to distribution terminals and then to pumps is assumed to be 110 miles<sup>82</sup> and is the same for the Py-ECH and CE systems. Diesel truck fuel economy (assumed to be 5 miles/gallon) and emissions were obtained from GREET.

### 3.4. Combustion

Greenhouse gas emissions for complete combustion of finished fuels were calculated for both processes. NO<sub>x</sub> emissions, contributing to eutrophication potential, were estimated using GREET for gasoline and ethanol for Py-ECH and CE systems, respectively.

### 3.5. Allocation of Agricultural Activities

Corn cultivation yields both corn grain and stover, thus the burdens and benefits due to cultivation, including below-ground carbon sequestration, must be allocated. Allocation is a challenging and important topic in LCA as it can lead to drastically differing results depending on how it is performed. LCA methodologies in the literature describe different ways to avoid allocation in multifunctional processes, including process subdivision or system expansion.<sup>83, 84</sup> If allocation cannot be avoided then burdens should be allocated based on some biological, physical, or chemical relationships that link the system functions to process inputs or outputs. If such a physical relationship cannot be established, then the allocation can be based on other factors such as economic value.

In the present analysis, allocation is only necessary in the cultivation stage of the two systems. Two allocation approaches were considered, (a) allocation method 1 with no allocation to stover (b) allocation method 2 with mass-based allocation. In Method 1, allocation was avoided based on the rationale that the corn stover is a waste product of corn grain production.<sup>85</sup> This assumption makes it possible to neglect any cultivation emissions or benefits that were shared with the corn grain, such as soil carbon sequestration. The only emissions attributed to stover cultivation in this method are from the production and application of additional fertilizers to offset nutrients removed with the harvested corn stover. In Method 2, mass-based allocation was performed when subdivision was not possible. The grain-to-stover mass ratio in a corn plant is approximately 1:1.<sup>86</sup> However, since only 60% of the corn stover is harvested and 40% is left on the fields, the mass-based stover allocation percentage was calculated as 34%, consistent with the value reported in GREET. Accordingly, 34% of the total fertilizer emissions and net soil carbon sequestration were allocated to stover in Method 2. The second-pass harvest emissions for stover (from GREET) were fully allocated to stover for both methods. Apart from cultivation, emissions from all other stages were the same in the two methods.

## 4. Results and Discussion

### 4.1. Life Cycle Impact Assessment (LCIA)

The LCIA phase of the LCA quantifies the environmental impacts of the various emissions that were compiled in the life cycle inventory phase. In this study, the LCIA was completed for three impact categories: greenhouse gas emissions (GHG), eutrophication potential (EUP), and water scarcity footprint (WSF). The total GHG emissions, EUP, and WSF for the Py-ECH and CE processes, employing both allocation procedures, are summarized in Tables S6 and S7 (in the Supplemental Information), respectively.

## 4.2. Contribution Analyses

### *GHG Emissions:*

GHG emissions were calculated and compared for each system and allocation method. Figure 3 shows the contributions of different system components of the two systems for both allocation methods. For the Py-ECH system, electricity for upgrading during ECH and hydroprocessing is assumed to come from either the MROW 2020 grid or a fully renewable source. When renewable electricity is used, the Py-ECH system performs slightly better than the CE system in terms of GHGs for the chosen functional unit of 1 MJ of fuel energy. However, if grid electricity is used for Py-ECH, the Py-ECH system has higher GHG emissions. This highlights the importance of low-carbon electricity in the Py-ECH system owing to the large amount of electricity utilized for fuel upgrading.

The amount of biomass feedstock (green bars) required is another significant different between both processes. The CE system has a lower liquid fuel energy yield than Py-ECH, i.e., it requires more biomass feedstock to make the same amount of fuel energy (in this analysis the functional unit is 1 MJ). As a result, the CE system has a greater benefit from biogenic carbon fixation per unit of fuel produced. It must be noted here that the fixed feedstock carbon is eventually emitted when combusting the liquid fuel (for Py-ECH/CE systems), during electricity and process heat generation, and CO<sub>2</sub> fermentation (exclusively for the CE system). Though there are increased emissions from harvesting, fertilizer application and fertilizer production to support a larger biomass input in the CE system, these emissions are very small relative to the amount of feedstock carbon being fixed. Additionally, there is more soil carbon sequestration (cyan colored bar) associated with generating larger quantities of corn stover to make the functional unit of 1 MJ of CE fuel energy.

The GHG contribution of the processing components for the two systems was subdivided into four sub-components: heat and power generation from biomass, electricity to/from the grid, fermentation CO<sub>2</sub>, and co-products. The contribution to heat and power generation from biomass (dark blue bars) is much greater for the CE system because of lignin and wastewater sludge combustion, while for the Py-ECH, these emissions are from heat production needed for pyrolysis. Also, for Py-ECH, the grid electricity (orange bars) required is the largest GHG emission when using the MRO grid. CO<sub>2</sub> generated by fermentation of holocellulose sugars (light blue bar) is an emission from the CE system that is not present in the Py-ECH system. The final sub-component is associated with co-products, which are excess electricity (renewable electricity that displaces fossil fuels in the grid electricity mix) sold to the grid for the CE system and biochar, which is land-applied for the Py-ECH system. As biochar sequesters carbon when land-applied, it has a negative value on Figure 3 (black bar). The biochar carbon reported is the net carbon sequestered (65 wt.% of total biochar carbon) after accounting for the carbon fraction eventually liberated as CO<sub>2</sub>. The combined emissions from the feedstock and fuel transport stages for both processes are negligible and are not visible in Figure 3. The emissions from fuel combustion, although not negligible, are nearly equal for both systems. The emissions associated with corn stover losses during harvesting, transport, and storage, are also minimal. Finally, there is little difference using different allocation methods within a single system as only a slight increase in all values results when using mass allocation (method 2) vs. treating stover as a waste (method 1).

Several LCAs involving pyrolysis, but without ECH, have been reported in the literature. In a study by Steele et al.,<sup>87</sup> the total GHG emissions in a cradle-to-grave analysis of forest residue into bio-oil for combustion to make electricity are about 32 g CO<sub>2</sub>/MJ. Though this is 63% less than our result for Py-ECH using grid electricity, the bio-oil is only combusted in boilers and not upgraded to transportation fuel. A second analysis in the same study for making residual fuel oil results in 107 g CO<sub>2</sub>/MJ, higher than the GHG emissions of Py-ECH even when using grid electricity. In a review of upgrading pyrolysis bio-oils by Sorunmu et al.,<sup>34</sup> with only one exception, all upgrading thermochemical processes have GHG emissions ranging between 5 and 60 g CO<sub>2</sub>/MJ. Only one scenario reported by Winjobi et al.<sup>88</sup> has GHG emissions as high as those of gasoline/diesel at about 93 g CO<sub>2</sub>/MJ. While most of these comparative processes have GHG emissions less than the Py-ECH system (using grid electricity), most upgrade bio-oil with either purchased hydrogen gas or syngas from the steam gasification of biochar. Finally, these previous



LCAs of biomass pyrolysis are for centralized bioenergy systems, characterized by locating all conversion equipment in a single large refinery. Py-ECH in this LCA was performed for a decentralized process, which uses ECH as a mild upgrading step at small-scale depots. The stabilized bio-oil is then transported and upgraded at a central facility that uses hydrogen made by wind- or solar-powered water electrolysis. While using grid electricity leads to GHG emissions towards higher values reported by Sorunmu et al.,<sup>34</sup> when using renewable electricity, Py-ECH has lower GHG emissions than all of these processes.

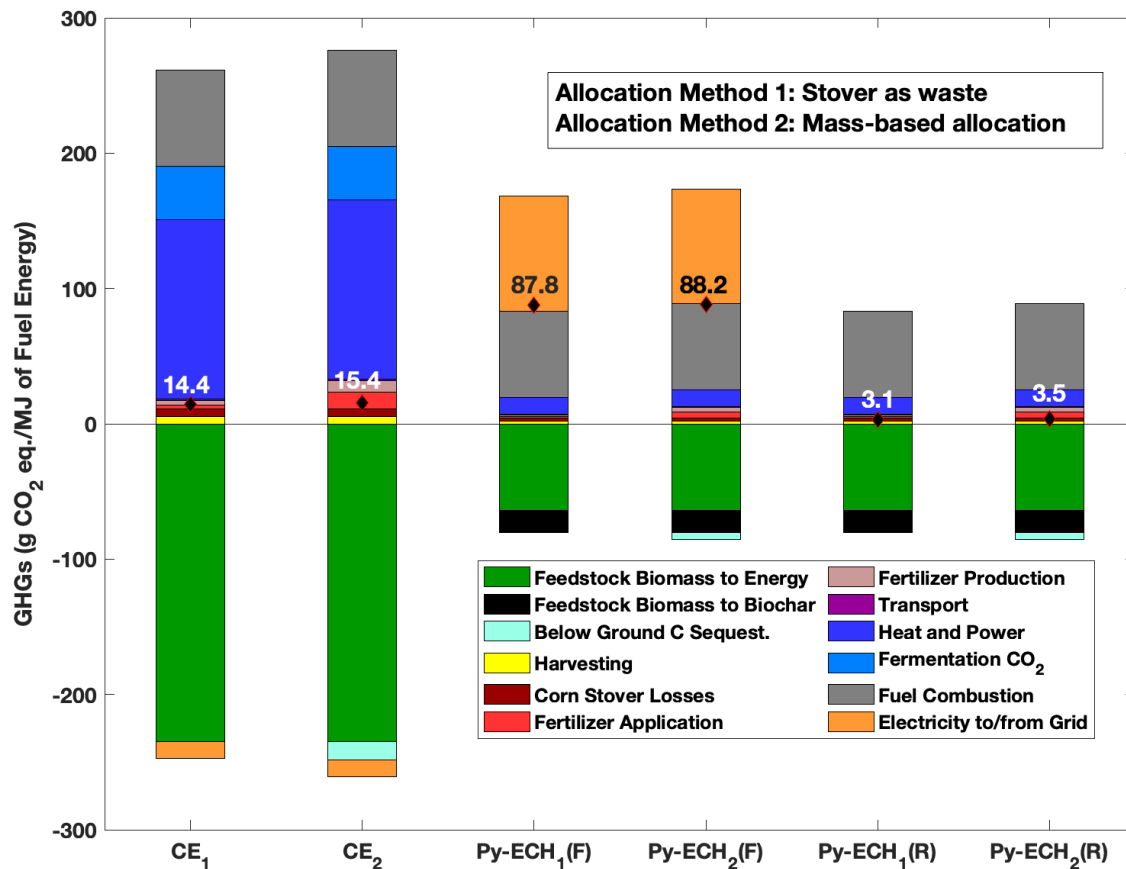


Figure 3: GHG results for cellulosic ethanol (CE) and pyrolysis electrocatalytic hydrogenation (Py-ECH) systems, without (subscript 1) and with (subscript 2) allocation of burdens to stover, using either 2020 MRO electrical grid which includes 70.8% fossil electricity (F) or fully renewable power (R). Diamond markers represent the net emissions.

### *Eutrophication Potential (EUP)*

The EUP contribution analyses are shown in Figure 4 for both systems, both allocation methods, and both Py-ECH electricity cases. As seen from Figure 4a, the cultivation-related components in

the two systems dominate EUP. The major cultivation contributors are the P and N runoff values. As for feedstock carbon fixation, the lower liquid fuel yield for CE results in greater nutrient runoff (per fuel energy produced) relative to Py-ECH. Fertilizer-related atmospheric emissions of NO<sub>x</sub> and NH<sub>3</sub> have negligible contributions. The contributions related to fuel production (denoted by blue and orange bars) for both systems are minimal, and not observable for the Py-ECH system. Fuel transport and combustion EUP are also negligible. To investigate the relative contributions of fuel production, transport, and fuel combustion, Figure 4b was constructed excluding the EUP contributions from cultivation. The CE refinery component has a high EUP in part because of greater NO<sub>x</sub> emissions from the boiler-combustor, which combusts a relatively large amount of fuel (lignin and wastewater sludge), considerably more than the combustors in the Py-ECH system (mixture of non-condensable gases (NCG) like CO, CO<sub>2</sub> and H<sub>2</sub> in depots and natural gas in refineries). Although the Py-ECH has additional emissions from utilization of grid electricity, the rate of NO<sub>x</sub> emissions is not nearly as high. The CE system also has atmospheric NH<sub>3</sub> emissions from its wastewater treatment plant. Fuel combustion EUP values are similar for both systems and allocation methods. Finally, the fuel transport emissions are negligible. Allocation assumptions, affecting only feedstock cultivation, have a larger impact on EUP values than on GHG emissions. For both allocation methods, Py-ECH has lower EUP than CE.

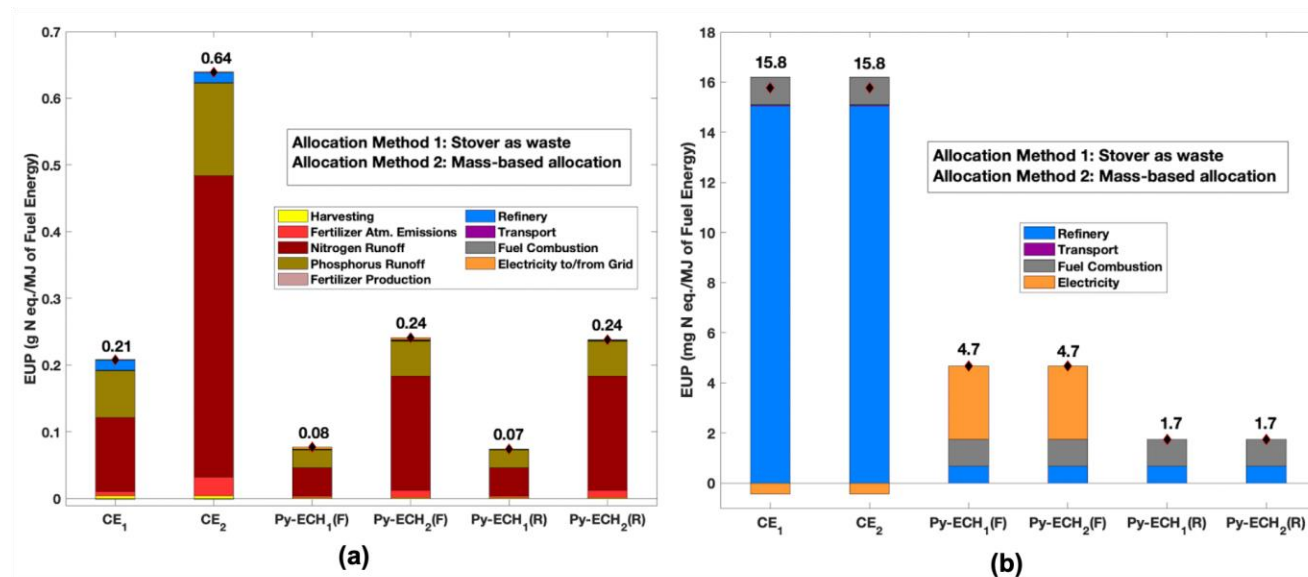


Figure 4: (a) EUP contribution analysis (b) EUP contribution analysis excluding cultivation and harvesting, for cellulosic ethanol (CE) and pyrolysis electrocatalytic hydrogenation (Py-ECH) systems, without (subscript 1) and with (subscript 2) allocation of burdens to stover, using either

2020 MRO electrical grid which includes 70.8% fossil electricity (F) or fully renewable power (R). Diamond markers represent the net emissions.

#### *Water Scarcity Footprint (WSF)*

The WSF results are shown in Figure 5 for both systems, both allocation methods, and both electricity-supply scenarios for Py-ECH. WSF is only relevant in two components of the two systems, feedstock cultivation and fuel production. There is no WSF contribution from fuel and biomass transportation and fuel combustion. The biggest contributor to WSF for both processes is cultivation (green bar), which includes freshwater consumption for agriculture but not precipitation, as discussed before. The water demand for cultivation for the CE system is much more than for the Py-ECH system, owing to the larger amount of biomass required to produce the same amount of fuel energy. Py-ECH requires water for ECH and electrolysis, however, the cooling tower make-up water requirement for the CE system is much larger (blue bars). When powered by grid electricity, the Py-ECH system consumes water because of water used at thermal power plants. The CE system has a small benefit due to excess electricity exported to the grid, thus reducing water consumption at thermal power plants. When Py-ECH is powered by grid electricity, its WSF is nearly the same as CE for the allocation method 1 assumptions (stover as waste). WSF is lower when the Py-ECH system uses only renewable electricity as water consumption for solar and wind power is much lower than in thermal power plants, as shown in Figure 5 (Py-ECH<sub>1</sub>—renewable electricity). Finally, the on-farm water consumption, which is the largest contributor, does not appear when using allocation method 1, which allocates all water consumption to corn grain, as stover is considered a waste product.

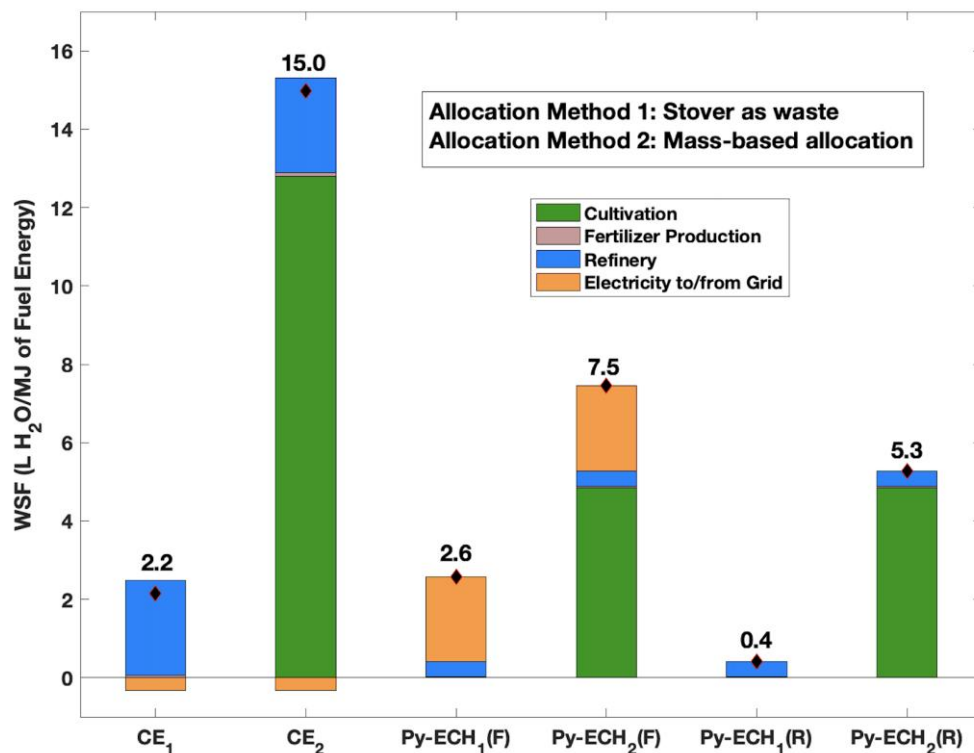


Figure 5: Water scarcity footprints cellulosic ethanol (CE) and pyrolysis electrocatalytic hydrogenation (Py-ECH) systems, without (subscript 1) and with (subscript 2) allocation of burdens to stover, using either 2020 MRO electrical grid which includes 70.8% fossil electricity (F) or fully renewable power (R). Diamond markers represent the net emissions.

### 4.3. Sensitivity Analyses

The contribution analyses reveal that the Py-ECH system is sensitive to the carbon intensity of the electricity used in the Py-ECH depots and central refinery. When using 2020 MROW grid electricity, which is 29% renewable, the GHG emissions for the Py-ECH system cannot match those of the CE system, which primarily uses renewable biomass for energy. However, when 100% renewable electricity is used, the Py-ECH system has lower life cycle GHG emissions. Figure 6 shows the dependence of GHG emissions on the renewable content of the grid electricity for both systems, using mass-based allocation. In contrast, the CE system, a net electricity producer, exhibits an increase in GHG emissions with grid electricity because less fossil electricity is displaced. Comparing the slopes in Figure 6, it is apparent that the Py-ECH system is more sensitive to the carbon intensity of the grid than the CE system. For the system

assumptions with mass-based allocation, the CE system performs better than the Py-ECH system when the renewable content in the electrical grid is below 87%. While the U.S. electrical grid is currently 20% renewable<sup>89</sup>, there are continued efforts to increase the deployment of renewable power sources.<sup>90-93</sup> The sensitivity analysis using “stover as waste” allocation, yields similar results.

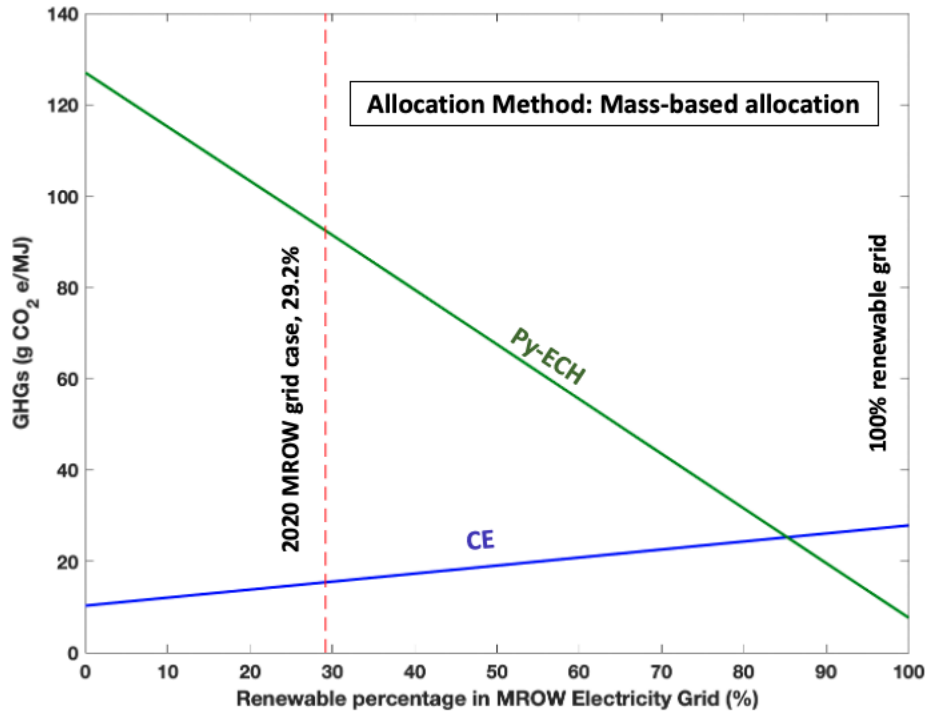


Figure 6: Sensitivity of lifecycle GHG emissions to the assumed % renewable content in grid electricity for allocation method 2. The 2020 MROW electricity grid has 29% renewable content, 100% is the completely renewable grid case, 87% is the crossover point where the two systems have equal GHG emissions.

Soil carbon sequestration during corn cultivation varies with soil texture, rainfall, tillage, stover removal, measured soil depth, crop rotation system, and geographical location. To investigate the sensitivity of total GHG emissions to soil carbon sequestration assumptions, the soil carbon sequestration was varied from 0 to 2.5 Mg C/ha/yr for the assumed continuous corn system, with no tillage, and 60% stover harvest. The limits were chosen to encompass the range of most literature estimates.<sup>52-58</sup> Figure 7, for the mass-based allocation method, shows that the CE system GHGs are more sensitive to the sequestration rate assumption than the Py-ECH system because more biomass feedstock is required per unit of fuel energy, resulting in greater sequestration. The

Py-ECH system with 2020 MROW grid electricity never has lower GHG emissions than the CE system, no matter what the annual C sequestration rate assumption. For reference, two sequestration values from the literature, indicated by red dashed lines, have been plotted in Figure 7. The first is from GREET and is used as the baseline value in the present analysis. The second is from Follett et al.,<sup>94</sup> who determined 1.3 Mg C/ha/yr for no-till corn stover when 50% is removed. Follett et al. measured soil carbon to depths of 150 cm, in contrast to most measurements that only sample to 30 cm. This is approximately equal to 1.1 Mg C/ha/yr for 60% removal, assuming a linear dependence and ignoring sequestration associated with root mass. Carbon sequestration rates above 0.4 yield fuels with net negative GHG emissions for both the CE and Py-ECH with renewable grid systems. For allocation method 1, with stover assumed to be a waste material, there is no sensitivity to sequestration rate, because all of the sequestration benefits accrue to the non-waste materials.

Because Py-ECH requires substantially less biomass and cultivation land area per unit of fuel produced, additional opportunities for GHG emission reductions are possible with the unused land (the incremental land area that would be required to produce the same amount of CE fuel). For example, if this incremental land could become natural forest and was included in the Py-ECH system boundary to equalize land area with the CE system, then Py-ECH (using renewable electricity) GHG emissions would be far lower than CE, as shown in Figures S2 and S3 in Supplementary Information. This would be true for all assumed values for carbon sequestration rate.

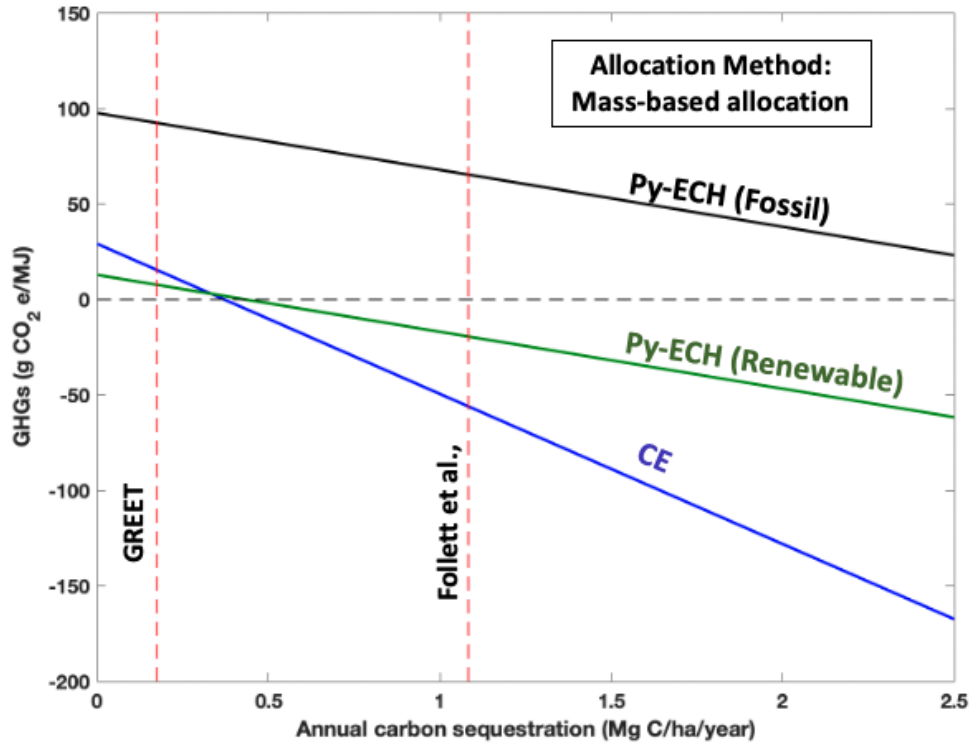


Figure 7: Sensitivity of GHG emissions to annual C sequestration rate for mass-based allocation.

#### 4.4. Energy Ratio

To compare energy efficiency of the two processes, five energy metrics were investigated to quantify the different aspects of energy efficiency of the Py-ECH and CE pathways.<sup>83</sup> The calculated ratio values, along with their descriptions are presented in Table 1.

Table 1: Energy ratios, along with their description,<sup>83</sup> for the CE and Py-ECH systems.

Energy Ratio	Abbreviation	Description	CE	Py-ECH (F)	Py-ECH (R)
Total Energy Ratio	ER <sub>t</sub>	Total usable energy output/ Total energy input	0.44	0.70	0.70
Energy Yield	E <sub>y</sub>	Fuel energy/Feedstock energy	0.42	0.91	0.91
Energy Return on Investment	EROI	Total energy of fuel and co-products/ Total energy input except feedstock	10.43	1.85	1.85

Renewability Factor	RF	Fuel energy output/ Fossil energy input	9.66	1.98	8.22
Fossil Energy Ratio	ER <sub>f</sub>	Total energy of fuel and co-products/ Fossil energy input	10.40	2.42	10.03

While the Total Energy Ratio (ER<sub>t</sub>) is a measure of the total efficiency of the system and accounts for both product and co-product energy, the Energy Yield (E<sub>y</sub>) only calculates the fraction of the feedstock energy residing in the primary fuel product. Therefore, the ER<sub>t</sub> includes the energy associated with excess hydrogen gas in the Py-ECH system and the excess electricity in the CE system. Biochar in the Py-ECH system is not considered an energy co-product since it is land applied to sequester carbon. As shown in Table 4, both of these ratios are higher for the Py-ECH system since it has a higher overall and fuel energy efficiency. There is no difference between the renewable and fossil electricity scenarios because these energy metrics do not differentiate between fossil and renewable energy.

EROI is similarly defined as ER<sub>t</sub>, with the exception that it does not include the energy associated with the biomass feedstock input. It accounts for the additional energy inputs to the process that are essential for manufacturing the fuel and the co-products. Table 4 shows that the EROI for the CE system is much higher as the majority of the energy input for the CE system comes from the biomass feedstock, which is not included in the denominator. The EROI does not distinguish between the renewability of energy sources and thus shows no difference in the two Py-ECH scenarios.

To determine the renewability of a system, energy parameters such as Energy Renewability Efficiency (ER<sub>f</sub>)<sup>83</sup> and Renewability Factor (RF) offer valuable insight. RF is the ratio of the energy of the primary product (the fuel in this case) and all non-renewable energy inputs. The higher the RF, the greater is the renewability of the system. ER<sub>f</sub> is the ratio of all energy products (fuel and co-products) and all fossil energy inputs. Therefore, the only difference between RF and ER<sub>f</sub> is that the former only accounts for the primary product whereas the latter accounts for co-products as well. It can be seen from Table 4 that the RF and ER<sub>f</sub> of the CE system is greater than for the Py-ECH system. This is because the CE system manufactures its own heat and power by combusting some of its biomass feed, thereby greatly reducing non-renewable inputs resulting in a larger RF and ER<sub>f</sub>. When renewable electricity is used for Py-ECH, RF and ER<sub>f</sub> increase



substantially due to lower fossil energy inputs. However, RF and  $ER_f$  for Py-ECH remain lower than the CE system because of the natural gas used to supply heat at the central refinery, which could be overcome if renewable heat is used (provided by burning additional biomass at the refinery). Figure 8 shows the fraction of renewable grid electricity needed for the renewability of the Py-ECH system to match the CE system under such a scenario. With completely renewable heat, the electricity grid must be 85-87% renewable for Py-ECH to match CE in terms of RF and  $ER_f$ . Similarly, if the electricity source is 100% renewable, the refinery's heat source would have to be at least 25% renewable (RF) and 5% renewable ( $ER_f$ ) for the Py-ECH system to match that of the CE system. The variation of the RF and  $ER_f$  with percentage renewable heat at the central refinery has been provided in the Supplementary Information.

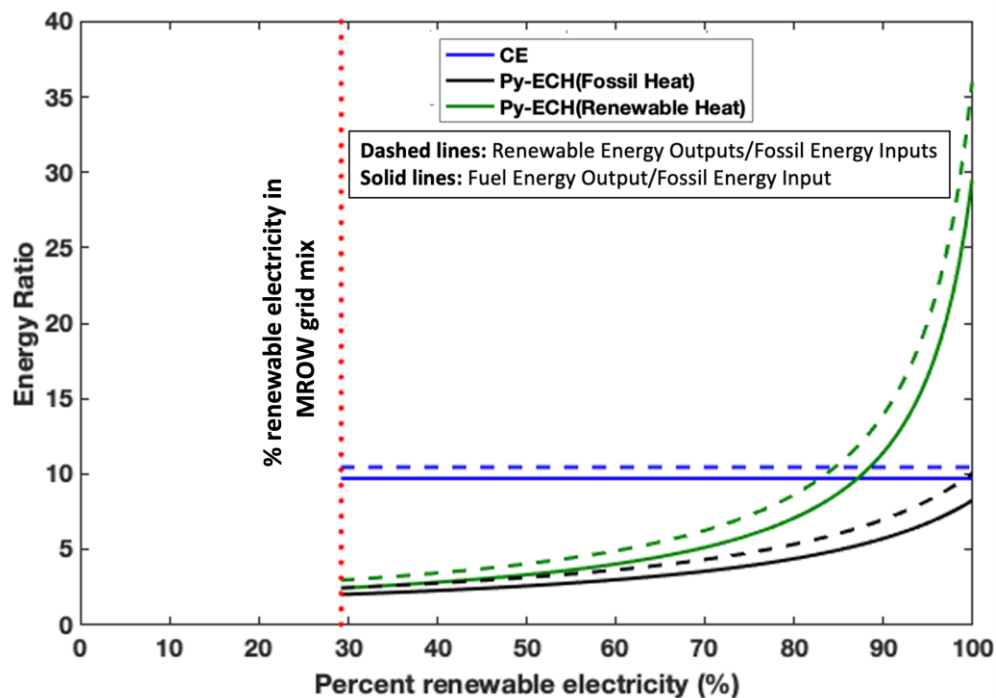


Figure 8: Sensitivity of system RF and  $ER_f$  to % renewable electricity. Fossil or renewable heat indicate that heat at central refinery is provided either from fossil (natural gas) or renewable sources.

#### 4.5. Alternative Functional Unit

A major takeaway from the present comparative life cycle assessment is the importance of renewable electricity used in the Py-ECH system. The GHGs from Py-ECH are greater or lower than those from the CE system depending upon the percentage renewability of the electrical grid.

Another key feature of this analysis is the selection of the functional unit. The “per MJ of fuel energy” basis, as assumed in this study, disadvantages the Py-ECH system in terms of the GHG emissions because its greater energy yield results in less biomass required than the CE system and consequently lower biogenic carbon fixation benefits. On the other hand, Py-ECH has lower eutrophication potential and water use, due to reduced corn stover cultivation and fertilizer use. By changing the functional unit to “kg corn stover processed,” the cultivation stages of the Py-ECH and the CE processes become identical. This functional unit results in greater fuel production in the Py-ECH system, owing to a greater fuel yield. GHG emissions for the two systems are greatly affected, which can be seen by comparing the results in Figure 9 for the stover-based functional unit to those of the fuel-based functional unit in Figure 3. Total biogenic carbon (feedstock carbon for CE and feedstock and biochar carbon for Py-ECH) is equal for both systems for the stover-based functional unit. When 100% renewable grid electricity is employed, the Py-ECH system has negative net GHG emissions because electricity usage is the primary contributor.

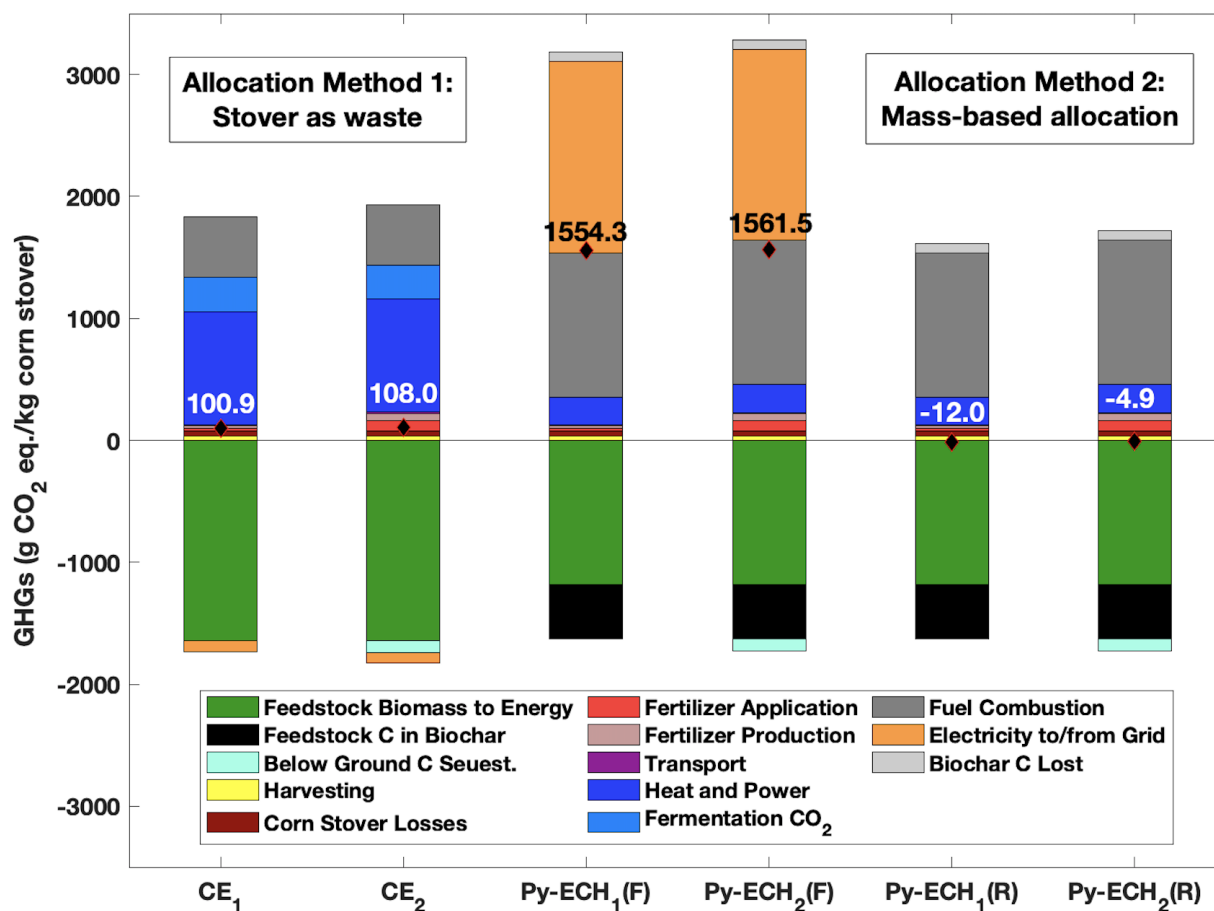


Figure 9: GHG results for cellulosic ethanol (CE) and pyrolysis electrocatalytic hydrogenation (Py-ECH) systems, without (subscript 1) and with (subscript 2) allocation of burdens to stover, using either 2020 MROW electrical grid which includes 70.8% fossil electricity (F) or fully renewable power (R). Diamond markers represent the net emissions.

## 5. Conclusion

We have previously shown that compared to microbial bioconversion via the CE system, the Py-ECH system enables significantly higher yields of renewable hydrocarbon fuels and potentially offers a large-scale mechanism for chemical storage of renewable but intermittently generated electrical energy as transportation fuel.<sup>11</sup> The climate change, eutrophication, and water scarcity impacts of liquid biofuels produced using the CE and Py-ECH systems are assessed here. Both CE and Py-ECH liquid biofuels have lower GHG emissions than gasoline from crude oil. GHG emissions for CE are 14-16% of gasoline, while emissions for liquid hydrocarbons using Py-ECH with existing grid electricity or 100% renewable electricity are 87-93% or 3-8% those of gasoline. The breakeven relative to CE occurs at ~87% renewable electricity, above which Py-ECH outperforms CE. In terms of water scarcity, Py-ECH performs similarly to CE using current grid electricity and considerably better when renewable electricity is used. The eutrophication potential for Py-ECH is lower than for CE for both electricity assumptions.

While the CE system is more energy intensive than the Py-ECH system on an overall basis, the fossil energy footprint is currently greater for the Py-ECH system. This is primarily due to the high dependence of the Py-ECH system on grid electricity, which is only 29% renewable (MROW electricity grid). Sensitivity analyses revealed that using completely renewable heat at the central refinery and ~87% renewable grid electricity lowers the fossil energy footprint of Py-ECH to below the CE process.

## Acknowledgements

This work was funded in part by the Ford Motor Company and the National Science Foundation under award number 2055068. Dr. Saffron's contribution was supported in part by the USDA National Institute of Food and Agriculture, Hatch project 1018335, and Michigan State University AgBioResearch.

## Author contributions:

Sabyasachi Das developed the methodology and process models, performed the formal analyses, and wrote the original draft of this manuscript. James Anderson, Robert De Klein, and Timothy Wallington developed the methodology for comparing scenarios, obtained funding resources, and edited the manuscript. James Jackson conceptualized the Py-ECH process and investigated its use to hydrogenate organic compounds. Chris Saffron conceptualized the Py-ECH process and this project, investigated its use, acquired funding, developed the methodology for comparison, supervised the project, and edited the manuscript.

## References

1. U. S. Congress, *Energy Independence and Security Act of 2007*, Washington, DC, 2007.
2. D. Humbird, R. Davis, L. Tao, C. Kinchin, D. Hsu, A. Aden, P. Schoen, J. Lukas, B. Olthof and M. Worley, *Process design and economics for biochemical conversion of lignocellulosic biomass to ethanol: dilute-acid pretreatment and enzymatic hydrolysis of corn stover*, Report NREL/TP-5100-47764, National Renewable Energy Laboratory (NREL), Golden, CO., 2011.
3. S. Chen, Z. Xu, X. Li, J. Yu, M. Cai and M. Jin, *Bioresource Technology*, 2018, **258**, 18-25.
4. J. Yu, Z. Xu, H. He, S. Chen, S. Wang, Y. Yu and M. Jin, *Biomass Conversion and Biorefinery*, 2021, DOI: 10.1007/s13399-021-01642-3.
5. S. S. Dhiman, A. David, V. W. Braband, A. Hussein, D. R. Salem and R. K. Sani, *Applied Energy*, 2017, **208**, 1420-1429.
6. C. Zhang, in *Alcohol Fuels: Current technologies and Future Prospect*, ed. Y. Yun, Intechopen, 2019, DOI: 10.5772/intechopen.86701.
7. P. Halder, K. Azad, S. Shah and E. Sarker, in *Advances in Eco-Fuels for a Sustainable Environment*, ed. K. Azad, Woodhead Publishing Series in Energy, 2018, ch. 8, p. 26.
8. Clariant, Ready for business: How Clariant is laying the ground for second-generation biofuels and much more, <https://www.clariant.com/en/Corporate/Blog/2021-Blog-Posts/12/First-commercial-sunliquid-plant>, (2021).
9. E. Ahmad and K. K. Pant, in *Waste Biorefinery*, eds. T. Bhaskar, A. Pandey, S. V. Mohan, D.-J. Lee and S. K. Khanal, Elsevier, 2018, DOI: <https://doi.org/10.1016/B978-0-444-63992-9.00014-8>, pp. 409-444.
10. M. Langholtz, *2016 Billion-Ton Report*, ORNL (Oak Ridge National Laboratory (ORNL), Oak Ridge, TN (United States)), 2016.
11. C. H. Lam, S. Das, N. C. Erickson, C. D. Hyzer, M. Garedew, J. E. Anderson, T. J. Wallington, M. A. Tamor, J. E. Jackson and C. M. Saffron, *Sustainable Energy & Fuels*, 2017, **1**, 258-266.
12. A. Inayat, A. Ahmed, R. Tariq, A. Waris, F. Jamil, S. F. Ahmed, C. Ghenai and Y.-K. Park, *Frontiers in Energy Research*, 2022, **9**.
13. Z. Li, M. Garedew, C. H. Lam, J. E. Jackson, D. J. Miller and C. M. Saffron, *Green Chemistry*, 2012, **14**, 2540.

14. M. Garedew, D. Young-Farhat, J. E. Jackson and C. M. Saffron, *ACS Sustainable Chemistry & Engineering*, 2019, **7**, 8375-8386.
15. M. Garedew, D. Young-Farhat, S. Bhatia, P. Hao, J. E. Jackson and C. M. Saffron, *Sustainable energy & fuels*, 2020, DOI: 10.1039/C9SE00912D.
16. M. Garedew, F. Lin, B. Song, T. M. DeWinter, J. E. Jackson, C. M. Saffron, C. H. Lam and P. T. Anastas, *ChemSusChem*, 2020, **13**, 4214-4237.
17. M. Garedew, C. H. Lam, L. Petitjean, S. Huang, B. Song, F. Lin, J. E. Jackson, C. M. Saffron and P. Anastas, *Green Chemistry*, 2021.
18. Y. Zhou, G. E. Klinger, E. L. Hegg, C. M. Saffron and J. E. Jackson, *Journal of the American Chemical Society*, 2020, DOI: 10.1021/jacs.0c00199.
19. C. H. Lam, C. B. Lowe, Z. Li, K. N. Longe, J. T. Rayburn, M. A. Caldwell, C. E. Houdek, J. B. Maguire, C. M. Saffron, D. J. Miller and J. E. Jackson, *Green Chem.*, 2015, **17**, 601-609.
20. Z. Li, S. Kelkar, L. Raycraft, M. Garedew, J. E. Jackson, D. J. Miller and C. M. Saffron, *Green Chemistry*, 2014, **16**, 844-852.
21. Y. Zhou, G. E. Klinger, E. L. Hegg, C. M. Saffron and J. E. Jackson, *Nature Communications*, 2022, **13**, 2050.
22. D. C. Elliott, *Energy & Fuels*, 2007, **21**, 1792-1815.
23. S. Das, J. E. Anderson, R. De Kleine, T. J. Wallington, J. E. Jackson and C. M. Saffron, *Sustainable Energy & Fuels*, 2022, **6**, 2823-2834.
24. A. Singh, D. Pant, N. E. Korres, A.-S. Nizami, S. Prasad and J. D. Murphy, *Bioresource Technology*, 2010, **101**, 5003-5012.
25. G. Z. Fu, A. W. Chan and D. E. Minns, *The International Journal of Life Cycle Assessment*, 2003, **8**, 137-141.
26. D. Mu, T. Seager, P. S. Rao and F. Zhao, *Environmental Management*, 2010, **46**, 565-578.
27. Y. Bai, L. Luo and E. van der Voet, *The International Journal of Life Cycle Assessment*, 2010, **15**, 468-477.
28. J. B. Dunn, S. Mueller, H.-y. Kwon and M. Q. Wang, *Biotechnology for Biofuels*, 2013, **6**, 51-51.
29. M. Wang, J. Han, J. B. Dunn, H. Cai and A. Elgowainy, *Environmental Research Letters*, 2012, **7**, 045905.
30. S. Kim, B. E. Dale and R. Jenkins, *The International Journal of Life Cycle Assessment*, 2009, **14**, 160-174.
31. S. Spatari, D. M. Bagley and H. L. MacLean, *Bioresource Technology*, 2010, **101**, 654-667.
32. A. Burnham, J. Han, C. E. Clark, M. Wang, J. B. Dunn and I. Palou-Rivera, *Environmental Science & Technology*, 2012, **46**, 619-627.
33. J. Han, A. Elgowainy, J. B. Dunn and M. Q. Wang, *Bioresource Technology*, 2013, **133**, 421-428.
34. Y. Sorunmu, P. Billen and S. Spatari, *GCB Bioenergy*, 2020, **12**, 4-18.
35. S. Kim, X. Zhang, A. D. Reddy, B. E. Dale, K. D. Thelen, C. D. Jones, R. C. Izaurralde, T. Runge and C. Maravelias, *Environmental Science & Technology*, 2020, **54**, 10797-10807.
36. M. Wang, *The Greenhouse Gases, Regulated Emissions, and Energy Use in Transportation Model*, Argonne National Laboratory, Argonne, Illinois, 1999.

37. J. B. Dunn, Z. Qin, S. Mueller, H. Y. Kwon, M. Wander and M. Wang, *Carbon Calculator for Land Use Change from Biofuels Production (CCLUB)*, Report ANL/ESD/12-5 Rev. 2, Argonne National Laboratory, 2014.
38. J. C. Bare, *Tools for the Reduction and Assessment of Chemical and Other Environmental Impacts (TRACI), Version 2.1-User's Manual*, United States Environment Protection Agency, 2012.
39. J.-B. Bayart, C. Bulle, L. Deschênes, M. Margni, S. Pfister, F. Vince and A. Koehler, *The International Journal of Life Cycle Assessment*, 2010, **15**, 439-453.
40. A.-M. Boulay, J. Bare, L. Benini, M. Berger, M. J. Lathuillière, A. Manzardo, M. Margni, M. Motoshita, M. Núñez, A. V. Pastor, B. Ridoutt, T. Oki, S. Worbe and S. Pfister, *The International Journal of Life Cycle Assessment*, 2018, **23**, 368-378.
41. E. Furimsky, *Applied Catalysis A: General*, 2000, **199**, 147-190.
42. B. Morelli, T. R. Hawkins, B. Niblick, A. D. Henderson, H. E. Golden, J. E. Compton, E. J. Cooter and J. C. Bare, *Environmental Science & Technology*, 2018, **52**, 9562-9578.
43. J. C. Bare, *Clean Technologies and Environmental Policy*, 2011, **13**, 687-696.
44. G. A. Norris, *Journal of Industrial Ecology*, 2002, **6**, 79.
45. B. P. Weidema and M. S. Wesnæs, *Journal of Cleaner Production*, 1996, **4**, 167-174.
46. M. W. Toffel and A. Horvath, *Environmental Science & Technology*, 2004, **38**, 2961-2970.
47. S. Couillard, G. Bage and J.-S. Trudel, *Comparative Life Cycle Assessment (LCA) of Artificial vs Natural Christmas Tree*, Report 1043-RF3-09, 2009.
48. S. Kim, X. Zhang, B. E. Dale, A. D. Reddy, C. D. Jones, K. Cronin, R. C. Izaurrealde, T. Runge and M. Sharara, *Biofuels, Bioproducts & Biorefining*, 2018, **12**, 203-212.
49. J. Rees, M. Schmer and C. Wortmann, Corn Stover Removal: Nutrient Value of Stover and Impacts on Soil Properties, <https://cropwatch.unl.edu/2017/corn-stover-removal-nutrient-value-stover-and-impacts-soil-properties>, (2018).
50. H. Xu, H. Sieverding, H. Kwon, D. Clay, C. Stewart, J. M. F. Johnson, Z. Qin, D. L. Karlen and M. Wang, *GCB Bioenergy*, 2019, **11**, 1215-1233.
51. R. Alvarez, *Soil Use and Management*, 2005, **21**, 38-52.
52. J. M. Baker, T. E. Ochsner, R. T. Venterea and T. J. Griffis, *Agriculture, Ecosystems & Environment*, 2007, **118**, 1-5.
53. B. Minasny, A. B. McBratney, V. Bellon-Maurel, J.-M. Roger, A. Gobrecht, L. Ferrand and S. Joalland, *Geoderma*, 2011, **167-168**, 118-124.
54. T. O. West and W. M. Post, *Soil Science Society of America Journal*, 2002, **66**, 1930-1946.
55. D. A. Angers and N. S. Eriksen-Hamel, *Soil Science Society of America Journal*, 2008, **72**, 1370-1374.
56. I. Virto, P. Barré, A. Burlot and C. Chenu, *Biogeochemistry*, 2012, **108**, 17-26.
57. W. Zhang, K. Liu, J. Wang, X. Shao, M. Xu, J. Li, X. Wang and D. V. Murphy, *Scientific Reports*, 2015, **5**, 10791.
58. R. Lal, W. Negassa and K. Lorenz, *Current Opinion in Environmental Sustainability*, 2015, **15**, 79-86.
59. A. Y. Hoekstra, A. K. Chapagain, M. M. Aldaya and M. M. Mekonnen, *The Water Footprint Assessment Manual: Setting the Global Standard*, Earthscan, 2011.
60. D. J. Lampert, H. Cai and A. Elgowainy, *Energy & Environmental Science*, 2016, **9**, 787-802.

61. S. Pfister, A. Koehler and S. Hellweg, *Environmental Science & Technology*, 2009, **43**, 4098-4104.
62. B. G. Ridoutt and S. Pfister, *Global Environmental Change*, 2010, **20**, 113-120.
63. S. Pfister and S. Hellweg, *Proceedings of the National Academy of Sciences*, 2009, **106**, E93-E94.
64. A. Y. Hoekstra, *Ecological Indicators*, 2016, **66**, 564-573.
65. IPCC, *Revised 1996 IPCC Guidelines for National Greenhouse Gas Inventories*, 1996.
66. S. E. Powers, *Quantifying Cradle-to-Farm Gate Life-Cycle Impacts Associated with Fertilizer Used for Corn, Soybean, and Stover Production* NREL, Golden, Colorado, 2005.
67. V. Smil, *Annual Review of Energy and the Environment*, 2000, **25**, 53-88.
68. W. Edwards, *Economics of Harvesting and Transporting Corn Stover* Iowa State University, 2014.
69. J. R. Hess, K. L. Kenney, C. T. Wright, R. Perlack and A. Turhollow, *Cellulose*, 2009, **16**, 599-619.
70. S. Sokhansanj, A. Turhollow and E. Wilkerson, *Resource Magazine*, 2008, **15**, 15-18.
71. Q. Li, H. Cai, J. Kelly and J. Dunn, *Expanded Emission Factors for Agricultural and Mining Equipment in GREET Full Life-Cycle Model*, Argonne National Laboratory, 2016.
72. I. Emery and N. Mosier, *GCB Bioenergy*, 2015, **7**, 865-876.
73. I. Emery, J. B. Dunn, J. Han and M. Wang, *BioEnergy Research*, 2015, **8**, 590-604.
74. K. Crombie, O. Mašek, A. Cross and S. Sohi, *GCB Bioenergy*, 2015, **7**, 1161-1175.
75. K. Crombie and O. Mašek, *Bioresource Technology*, 2014, **162**, 148-156.
76. K. Sun, J. Jin, M. Keiluweit, M. Kleber, Z. Wang, Z. Pan and B. Xing, *Bioresource Technology*, 2012, **118**, 120-127.
77. B. A. Oni, O. Oziegbe and O. O. Olawole, *Annals of Agricultural Sciences*, 2019, **64**, 222-236.
78. A. Panagopoulos, K.-J. Haralambous and M. Loizidou, *Science of The Total Environment*, 2019, **693**, 133545.
79. J. McGill and M. Darr, *Transporting Biomass on Iowa Roadways* Iowa State University, 2014.
80. S. Das and C. M. Saffron, *ECS Meeting Abstracts*, 2019, **MA2019-02**, 1041-1041.
81. S. Kim, X. Zhang, B. E. Dale, A. D. Reddy, C. D. Jones and R. C. Izaurralde, *Biofuels, Bioproducts and Biorefining*, 2018, DOI: <https://doi.org/10.1002/bbb.1899>.
82. D. Kumar and G. Murthy, *The International Journal of Life Cycle Assessment*, 2012, **17**, 388-401.
83. F. Dias Mayer, M. Brondani, M. Carrillo, R. Hoffmann and E. Lora, *Journal of Cleaner Production*, 2019, **252**, 119850.
84. L. Luo, E. van der Voet, G. Huppes and H. A. Udo de Haes, *The International Journal of Life Cycle Assessment*, 2009, **14**, 529-539.
85. J. Sheehan, A. Aden, K. Paustian, K. Killian, J. Brenner, M. Walsh and R. Nelson, *Journal of Industrial Ecology*, 2003, **7**, 117-146.
86. S. Sokhansanj, A. Turhollow, J. Cushman and J. Cundiff, *Biomass and Bioenergy*, 2002, **23**, 347-355.
87. P. Steele, M. E. Puettmann, V. K. Penmetsa and J. E. Cooper, *Forest Products Journal*, 2012, **62**, 326-334.

88. O. Winjobi, W. Zhou, D. Kulas, J. Nowicki and D. R. Shonnard, *ACS Sustainable Chemistry & Engineering*, 2017, **5**, 4541-4551.
89. B. Tyra, *Electric Power Monthly : U.S. electric net generation*, U.S. Energy Information Administration, 2022.
90. T. Mai, D. Mulcahy, M. M. Hand and S. F. Baldwin, *Energy*, 2014, **65**, 374-386.
91. P. Denholm, D. J. Arent, S. F. Baldwin, D. E. Bilello, G. L. Brinkman, J. M. Cochran, W. J. Cole, B. Frew, V. Gevorgian, J. Heeter, B.-M. S. Hodge, B. Kroposki, T. Mai, M. J. O'Malley, B. Palmintier, D. Steinberg and Y. Zhang, *Joule*, 2021, **5**, 1331-1352.
92. T. Mai, M. M. Hand, S. F. Baldwin, R. H. Wiser, G. L. Brinkman, P. Denholm, D. J. Arent, G. Porro, D. Sandor and D. J. Hostick, *IEEE Transactions on Sustainable Energy*, 2013, **5**, 372-378.
93. M. Bazilian, T. Mai, S. Baldwin, D. Arent, M. Miller and J. Logan, *Energy Strategy Reviews*, 2014, **2**, 326-328.
94. R. F. Follett, K. P. Vogel, G. E. Varvel, R. B. Mitchell and J. Kimble, *Bioenergy Research*, **4**, 866-875.